PNAS Nexus, 2026, **5**, pgag267
https://doi.org/10.1093/pnasnexus/pgag267
Published: 5 August 2026
Research report

One rule does not fit all: Deviations from universality in human mobility modeling

Ludovico Napoli[1], Márton Karsai[1,2], and Esteban Moro[3,4]*

[1]Department of Network and Data Science, Central European University, Quellenstraße 51, Vienna 1100, Austria
[2]National Laboratory for Health Security, HUN-REN Alfréd Rényi Institute of Mathematics, Reáltanoda utca 13-15, Budapest 1053, Hungary
[3]Media Lab, Massachusetts Institute of Technology, 75 Amherst St Cambridge, MA 02139, USA
[4]Network Science Institute, Department of Physics, Northeastern University, 177 Huntington Ave, Boston, MA 02115, USA
*To whom correspondence should be addressed: Email: e.moroegido@northeastern.edu
Edited By Wen-Dong Li

Abstract

Accurately modeling of individual movement in cities has significant implications for policy decisions across various sectors. Existing research emphasizes the universality of human mobility, positing that simple models can accurately capture population-level movements. However, population-level accuracy can mask structured heterogeneity at the individual level and does not guarantee consistent performance across all individuals. By overlooking individual differences, universality laws may accurately describe certain groups while less precisely representing others, resulting in systematic biases at the individual level. Using large-scale mobility data, we assess accuracy at individual level of a universal model, the Exploration and Preferential Return (EPR) model, by examining deviations from expected behavior in two scaling laws—one related to exploration and the other to return patterns. Our findings reveal that, while the model can accurately describe population-wide movement patterns, it displays widespread deviations linked to behavioral traits, socioeconomic and lifestyles of individuals, which are not fully captured by the model's assumptions. In particular, individuals poorly represented by the EPR model exhibit bursty exploration and sequential routine behaviors, associated with stronger temporal irregularity and habitual repetition. Among socioeconomic factors, income emerges as the strongest predictor of deviations from the model, leading to significant spatial disparities in accuracy. Notably, the universal accuracy of the EPR model deteriorates in urbanized and densely populated areas, underscoring essential policy implications. Our results show that reliance on universal mobility models may lead to uneven predictive performance across socioeconomic groups, particularly for vulnerable populations whose mobility patterns diverge most from model assumptions.

Keywords human mobility, inequalities, modeling, data, socioeconomic status

Significance Statement

Human mobility models are vital for understanding urban dynamics and informing transportation, infrastructure, and public health policies. While universal models like the Exploration and Preferential Return offer insights into population-wide movement patterns, our research shows that aggregate accuracy can mask structured individual-level heterogeneity, with model performance varying significantly across socio-demographic groups. By analyzing large-scale mobility data, we reveal that this model poorly represents individuals with lower incomes and more constrained routines. These systematic differences in model performance may lead to uneven predictive accuracy across socioeconomic groups when such models are used in policy-making contexts. Our findings highlight the importance of incorporating behavioral heterogeneity and urban context when interpreting and applying universal mobility models in transportation, infrastructure, and public health.

Introduction

As the global urban population continues to rise, cities play an increasingly pivotal role in societal development and daily life. This demographic shift amplifies the need for a deep understanding of human mobility within urban environments. Effective modeling of city movements is crucial not only for urban planning (1) and infrastructure development (2) but also for enhancing public

Received: December 1, 2025. **Accepted:** June 26, 2026

services (3), alleviating traffic congestion (4, 5), fostering social integration (6, 7), and controlling the spread of epidemics (8, 9).

Human mobility models (10) often seek to identify and replicate universal laws governing movement patterns. These include the distribution of travel distances (11, 12), the scaling of mobility flows with distance and population size (13, 14), and the spatiotemporal dynamics of aggregate movements (15). While these models have made significant strides in replicating observed aggregated behavioral patterns, their universal applicability remains uncertain across diverse populations. Rather than just mathematical exercises, mobility models must account for the reality that universality often comes at the cost of overlooking individual and group-level diversity. As a result, aggregate universality may mask structured heterogeneity in mobility behavior. Addressing this issue is essential to better understand the limitations and uneven performance of mobility models across different population groups and to support more inclusive urban planning and policy-making.

Over the years, various universal approaches have been proposed to model human mobility at both population and individual levels. At the macro level, mobility models often rely on the gravity (13, 16, 17) and radiation (14) laws to predict movements between meta-populations. At the individual level, random walk-based inspired models (11, 18) have been employed, assuming that humans behave like randomly moving particles (19). The Exploration and Preferential Return (EPR) model (20) stands out among individual mobility models due to its simplicity and ability to replicate key scaling laws observed in human mobility. By assuming lower stochasticity in human trajectories, this model increases predictability (21, 22) by focusing on two primary mechanisms: people explore new places less frequently over time and revisit highly visited locations more often. Due to its robustness, the EPR model has inspired extensions incorporating factors such as physical constraints (23), recency effects (24), ranking mechanisms (25), place relevance (26), routine behaviors (27), and social preferences (6).

However, despite allowing for individual variability in parameters, the model still relies on common underlying mobility mechanisms shared across individuals, overlooking variations in mobility patterns across different socioeconomic groups and lifestyles. For instance, socioeconomic status influences daily travel distance (28–30), travel frequency (31), the socioeconomic profile of visited locations (6, 32, 33), and the ability to adjust mobility during emergencies (34–37). Additionally, people visit places according to identifiable activity behaviors and lifestyles that span across sociodemographic groups (38). These differences are reflected in well-established heterogeneities in mobility patterns, including variations in routine behavior, temporal irregularity, and activity diversity (28, 39, 40). The EPR model can incorporate some of these factors by making its paramaters dependent on individual descriptors. Yet, the model still relies on common underlying exploration and return mechanism across individuals, potentially overlooking systematic behavioral diversity in the way people explore the city and return to their preferred places.

In this article, we aim to evaluate the performance of the EPR model mechanisms at the individual level. Our focus is on the scaling laws related to exploration dynamics and visitation frequencies. Specifically we assess whether the model represents the mobility of individuals with different behavioral characteristics equally well. Our analysis reveals a broad range of deviations from the model's expectations, associated with behavioral patterns that are not fully captured by its microscopic assumptions. We investigate the types of places visited when these assumptions are violated and the sociodemographic and lifestyle characteristics of individuals who deviate most from the model. Finally, we discuss the key implications of our findings, highlighting how aggregate universality can coexist with systematic and socially stratified differences in individual-level model performance.

Results

To address our scientific challenge, we analyze the microscale movements of 1.5 million anonymized users in 11 core-based statistical areas (41) (CBSAs) in the United States, recorded between October 2016 and March 2017. These data are extracted from a device-level dataset of high-resolution privacy-preserving mobile location pings for 4.5 million devices (for details on the raw data and cleaning process, see Materials and methods). For each user, we have a list of fine-grained spatially and temporally localized visits, each associated with a Foursquare venue and its category classification (42). In the following analysis, we focus on a subsample of 51,648 users from the Boston–Cambridge–Newton CBSA (referred to as Boston for simplicity). The analysis of other CBSAs can be found in the Supplementary material. Additional analyses on data representativeness, income-balanced resampling, and robustness to sampling biases are also reported in the Supplementary material.

Individual level deviations

In the framework of the Exploration and Preferential Return (EPR) model, users move between locations. At each step, a user u can either return to a previously visited place (return step) or explore a new place (exploration step). The individual tendency of a user u to explore, given that they have already visited S distinct locations is embedded in the exploration probability $P_u(S) = \rho_u S^{-\gamma}$. This probability is controlled by the individual parameter ρ_u, which is derived from the total number of distinct places visited by u compared to the total number of visits (see Materials and methods for details). With probability $1 - P_u(S)$ the user returns to an already location with probability proportional to the fraction of visits the user has made to that location. The parameter $\gamma = 0.22$ has been computed on the same dataset and for the same sample of users in (6), and it is fixed for all users. Note that similar values of γ were obtained for other different datasets (20).

The EPR model accurately reproduces two key aspects of human mobility: exploration dynamics and visitation frequency, at least on average. For exploration dynamics, the model assumes that exploration events happen stochastically in time. Thus, we focus on the inter-event time $\tau_{u,S}$, which we define as the number of steps after which a user u visits a new location, given that they have already visited S distinct places. According to the model (see Materials and methods for details), the expected inter-event time $\langle \tau_{u,S} \rangle$ is given by $\langle \tau_{u,S} \rangle = P_u^{-1}(S) = S^{\gamma}/\rho_u$. Meanwhile, a consequence of the preferential return mechanism is that the visitation frequency to the kth most visited location by a user u follows a universal Zipf's law, where $\langle f_{u,k} \rangle \sim k^{-\gamma}$.

If we average $\tau_{u,S}$ or $f_{u,k}$ among users in our data, as seen in panels Fig. 1A and D, the EPR model accurately reproduces

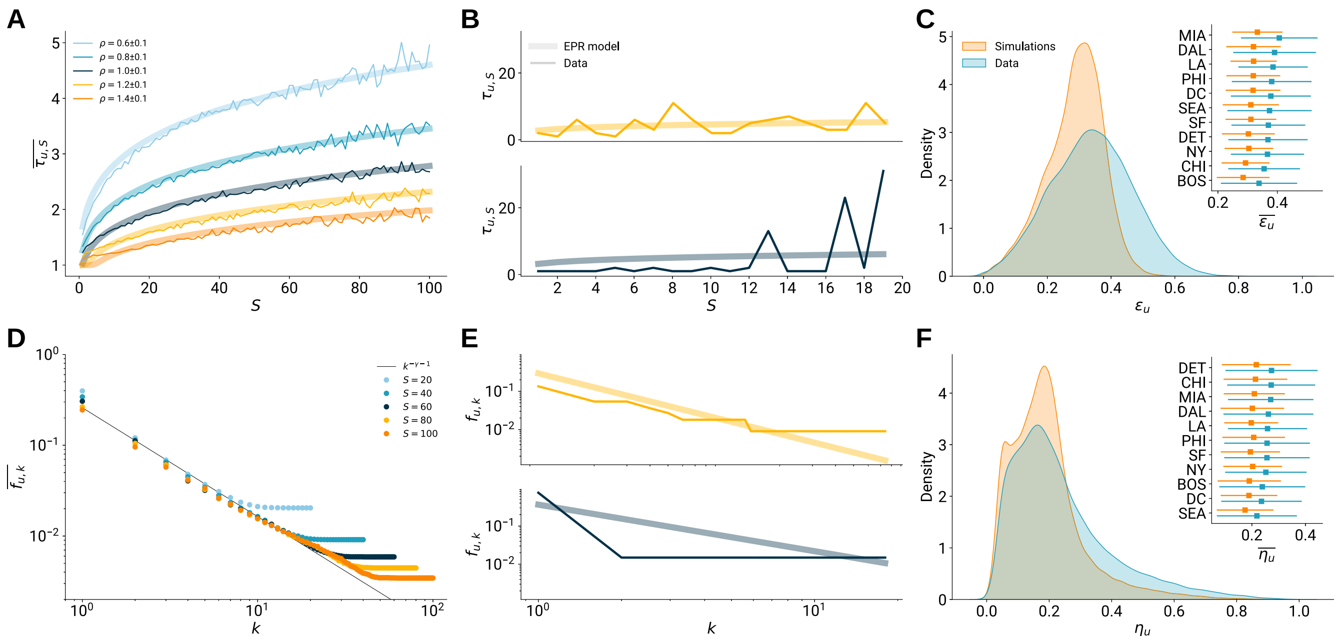

Figure 1 Individual deviations beyond population-wide accuracy. A) The average exploration inter-event time as a function of the number of distinct places S for users with different values of ρ_u (thin lines) and the corresponding predictions by the EPR model (thick lines). B) Individual-level observations of exploration inter-event time as a function of S (thin lines) and the predictions of the EPR model (thick lines) for two example users who visited 20 distinct places and that show, respectively, well-fitting (upper panel) and deviating (lower panel) behavior compared to the model. C) Distribution of individual deviations ϵ_u from the data and from stochastic simulations of the EPR model. The inset shows the mean and SD of the same distributions across all CBSAs. D) Average visitation frequency of ranked locations according to the EPR model (line) and for users with different values of S. E) Same as B) but for visitation frequency. F) Same as E) but for η_u.

both the exploration inter-event time and the visitation frequency. Nevertheless, looking at the individual level, by measuring these properties for each user separately, strong deviations appear for certain people from their predicted behavior.

For demonstration, Fig. 1B and E (upper panels) show an example of a user whose $\tau_{u,S}$ and $f_{u,k}$ adhere well to the scaling laws. In contrast, Fig. 1B and E (lower panels) illustrate the same metrics for a user whose behavior deviates from the predicted scaling. To quantify this effect, we introduce two individual metrics. To detect deviations from the exploration inter-event times, we define ϵ_u as the symmetric mean absolute percentage error (SMAPE) between $\tau_{u,S}$ and $\langle\tau_{u,S}\rangle$ for a user u:

$$\epsilon_u = \frac{1}{S_u}\sum_{S=1}^{S_u}\frac{|\tau_{u,S} - \langle\tau_{u,S}\rangle|}{|\tau_{u,S}| + |\langle\tau_{u,S}\rangle|},$$

where S_u is the total number of distinct places the user u visits. For the visitation frequency, η_u is defined as the Kullback–Leibler divergence between distributions $f_{u,k}$ and $\langle f_{u,k}\rangle$:

$$\eta_u = \sum_{k=1}^{K_u} f_{u,k}\log\frac{f_{u,k}}{\langle f_{u,k}\rangle},$$

where K_u is the rank of the least visited location (excluding locations visited only once, to remove the tail effect visible in Fig. 1B). To assess if deviations are due to the stochasticity, we compute both metrics for real and simulated mobility trajectories generated by the EPR model.

The distributions of ϵ_u and η_u for real and simulated users in the Boston area are shown in Fig. 1C and F, respectively. To facilitate comparison between the two variables (which is necessary for subsequent analysis), we normalize them to a range between 0 and 1. These distributions reveal that, while the EPR model reproduces the exploration dynamics and visitation frequency well on average, it does not equally represent the behavior of every user. Notably, the observed deviations are not solely due to the stochastic nature of the model. The orange distributions in Fig. 1C and F show the equivalent results from stochastic EPR model simulations for the same set of users (see the Supplementary material for details). Although stochasticity partially accounts for the observed variance (particularly for η_u), significant differences remain, particularly for the largest deviations, which cannot be explained by the model's stochastic variation alone. This observation holds not only for Boston but for every CBSA considered, as demonstrated in the subpanels of Fig. 1C and F, which display the mean and standard deviations of the real and simulated distributions of ϵ_u and η_u across all CBSAs.

Interestingly, despite measuring different mobility properties, the two deviation metrics show a strong correlation (Pearson correlation of 0.75), suggesting that a similar set of users systematically deviates from the model expectations in both dimensions. Using Monte Carlo significance tests against stochastic EPR realizations, we find that between ∼14 and 21% of users across CBSAs exhibit statistically significant deviations simultaneously in both dimensions (see Supplementary material).

Microscopic mechanisms

Given that some individuals show strong deviations from the EPR model, we aim to identify the mobility aspects that the model overlooks due to its assumptions and how these omissions contribute to poor demographic representativity.

First, one source of the deviations can be related to the individual exploration tendency, encoded in the parameter ρ_u. It controls the stochastic part of both ϵ_u and η_u, thus it partially explains their observed distributions even for simulations shown in Fig. 1C and F (for details, see Supplementary material). Nevertheless, while the exploration tendency is already integrated into the EPR model, we can use it as a control variable to rule out its stochastic effects on the deviations, when we focus on characteristics or mechanisms that the model fails to capture.

Regarding the inter-event times between consecutive explorations, the EPR model assumes that the probability of exploration decreases uniformly as the number of distinct visited places grows, according to the relation $P_u(S) = \rho_u S^{-\gamma}$. This assumption, however, does not explicitly account for burstiness, i.e. the interplay between long periods of low activity and short periods of high activity, a widely observed phenomenon in human dynamics (43). We hypothesize that users who exhibit more bursty exploration dynamics, will have a higher ϵ_u. These users exhibit a stronger tendency toward a microscopic feature that is not fully captured by the EPR model and is closely related to the inter-event time $\tau_{u,S}$.

To test this hypothesis, we measure the *exploration burstiness* as the parameter defined in Ref. (44) for each user (see Materials and methods for details) and analyze its relation with ϵ_u, while controlling for stochastic uncertainty via ρ_u. While conceptually related to established measures of temporal irregularity and activity variability (40, 43) (see Supplementary material), exploration burstiness specifically quantifies the intermittency of exploration events within individual mobility trajectories. The results are shown in Fig. 2A, where we group users into quantiles of ρ_u and exploration burstiness and compute the average ϵ_u within each group. This parameter space reveals that, beyond the ρ_u dependency, ϵ_u is positively associated with exploration burstiness. In fact, when considering a sample of users with the same exploration tendency, the more bursty users tend to be less well-represented by the EPR model in terms of their exploration dynamics. This association remains qualitatively stable after stratifying users by total activity volume (see Supplementary material).

The microscopic mechanism leading to the distribution $\langle f_k \rangle \sim k^{-\gamma}$ of visitation frequency in the EPR model is the preferential return criterion. This is a widely observed and modeled phenomenon in human systems (45), though it may not equally describe the behavior of all individuals. According to this criterion, the probability Π_i of visiting location i is equal to the fraction of visits ϕ_i the user has made to that location up to the point of observation. Our hypothesis is that the less a user follows this criterion, the less their visitation frequency distribution will align with the $\langle f_k \rangle \sim k^{-\gamma}$ scaling.

To test this hypothesis, we define the *biased return* as the SMAPE between Π_i and ϕ_i for each user (for details, see Materials and methods). Unlike burstiness-related measures, biased return is only weakly correlated with established mobility metrics related to recency and routine, such as immediate-return rates, visitation entropy, and activity-space concentration measures (39, 40) (see Supplementary material). This suggests that biased return captures a more specific deviation from the preferential-return mechanism itself. Similar to the case of exploration burstiness, to measure the biased return, we group users into quantiles of ρ_u and biased return, and compute the average η_u deviation within each group. As shown in Fig. 2B, the deviation η_u is positively associated with biased return, in addition to its expected dependence on ρ_u, especially for the lowest values of ρ_u. Specifically, for users with similarly low exploration tendencies, the more their mobility patterns deviate from the preferential return assumption, the less their visitation frequency distribution aligns with the EPR model's expected outcome of $\langle f_k \rangle \sim k^{-\gamma}$. Conversely, for highly explorative users, adherence to the preferential return mechanism does not seem to strongly influence the accuracy of the visitation frequency predicted by the EPR model.

To determine whether these observations are generalizable to other locations, we repeated our analysis for all CBSAs. As it turns out (see Supplementary material for details), the roles of exploration burstiness and biased return in determining the deviations ϵ_u and η_u are robust and consistent across all CBSAs analyzed.

Behavioral characterization of microscopic mechanisms

After assessing the direct and individual-level relationship between deviations from scaling laws and violations of the EPR model's assumptions, we aim to characterize these violations from a behavioral perspective. In other words, we want to investigate what types of places people visit when they deviate from the predicted exploration dynamics of the EPR model, instead engaging in bursty exploration periods. Similarly, where do people tend to return when they their mobility patterns deviate from the preferential return criterion?

As previously mentioned, we can address these questions because every step in our dataset is associated with a Foursquare venue with its own category and one of 13 macro taxonomy groups (see Materials and methods and Supplementary material for details), such as *Coffee/Tea, Grocery*, and *Shopping*. To characterize exploration burstiness, we analyze the taxonomy of bursty exploration trains, i.e. the place categories most likely visited during sequences of consecutive exploration steps (see Materials and methods for details). More specifically, we compare the frequency of visits to a given macro-category with its overall frequency of visits, as well as its frequency of visits during exploration steps only. Both comparisons are important: the first tells us how much more or less a category is visited during bursty trains compared to any other step, while the second restricts the comparison to exploration steps only, as specific categories may generally be visited more frequently during exploration but not necessarily during bursty periods. We measure both these relative frequencies for all the 13 taxonomy groups to characterize what places people visit more likely when they explore in a bursty manner.

As shown in Fig. 2C, bursty trains are indeed characterized by specific categories. In particular, amusement places such as museums and art galleries, coffee shops, and shopping locations are visited significantly more often during bursty exploration trains. Conversely, routine locations such as colleges and workplaces are rarely explored during bursty trains. Additionally, the macro category *City/Outdoor*, which comprises parks, neighborhoods, and residential places, is typically not explored in a bursty manner. The other categories show either small or diverging differences with respect to the comparisons considered.

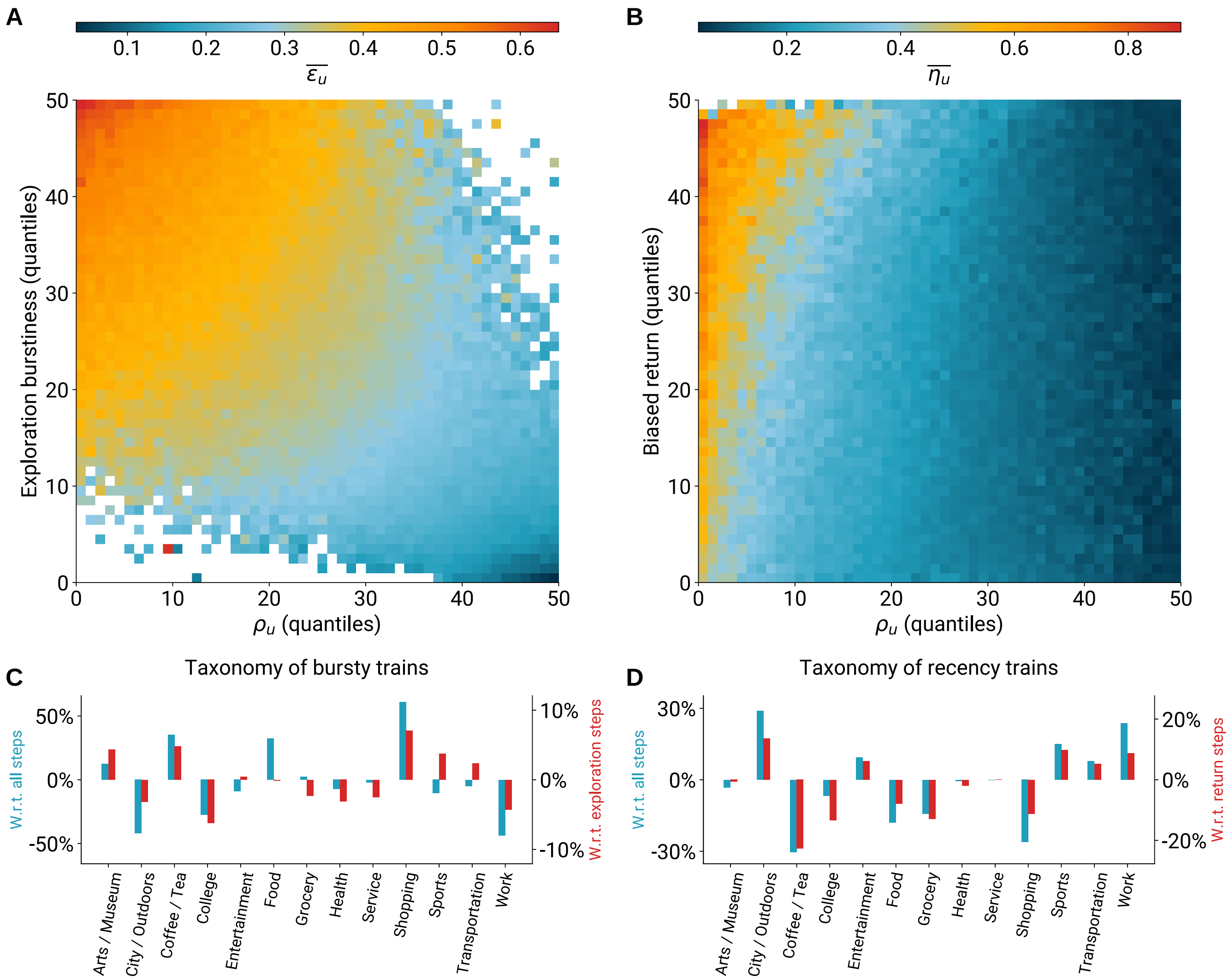

Figure 2 Deviations are related to violations of the EPR model's microscopic mechanisms. A) Average values of the deviation ϵ_u (color-coded as in the color bar) for users grouped in quantiles of ρ_u and exploration burstiness. Controlling for stochasticity with ρ_u, ϵ_u increases with burstiness. B) Average values of the deviation η_u (color-coded as in the color bar) for users grouped in quantiles of ρ_u and biased return. Controlling for stochasticity with ρ_u, η_u increases with biased return. C) Characterization of exploration bursty trains, i.e. sequences of consecutive exploration steps, in terms of relative visits to defined categories, compared to all visits (blue bars, left *y*-axis) and to exploration steps only (red bars, right *y*-axis). D) Characterization of recency trains, i.e. sequences of consecutive visits to the same place, in terms of relative visits to defined categories, compared to all visits (blue bars, left *y*-axis) and to return steps only (red bars, right *y*-axis).

Regarding biased return, recency has been identified and observed as one of the phenomena that characterize human mobility and is not captured by the original EPR model formulation (24). Recency describes a memory effect, indicating that humans tend to return not only to highly visited locations but more frequently to those visited recently, and is closely related to short-term memory and path-dependence effects (see Supplementary material). In contrast, the preferential return criterion does not account for this effect, assuming that all locations can be revisited based solely on their past frequency of visits, without considering the temporal order of those visits. To capture this effect while drawing a parallel with bursty trains, we introduce the concept of recency trains, i.e. sequences of consecutive return visits to the same place. Importantly, recency trains capture short-term sequential persistence in mobility behavior rather than generic long-term routine or visitation frequency concentration. We characterize these recency trains using the same methodology applied to bursty exploration trains. Specifically, we compare the frequency of visits to a given category with both its overall frequency and, in this case, its frequency during return steps only.

The results are shown in Fig. 2D, where we observe a somewhat mirrored pattern compared to bursty trains. When people repeatedly return to the same place, they tend to do so at routine and habitual locations, such as residential areas, workplaces, as well as transportation hubs and sports venues. In contrast, amusement places like coffee shops, restaurants, and shopping malls are not typically revisited continuously. Interestingly, entertainment places also appear in recency trains, though not significantly. It is also surprising that routine categories such as *College* and *Groceries* are notably absent from recency trains. This suggests that recency trains do not simply capture generic routine behavior, but rather short-term sequential persistence at the level of individual venues. Importantly, the analysis is relative in nature: categories are compared against both their overall visitation frequency and their visitation frequency during return steps more generally. Therefore, the absence of strong overrepresentation in recency trains does not imply that categories such as groceries or colleges are not recurrent or routine destinations. Rather, recurrent activities such as grocery shopping or university-related mobility may still constitute highly regular routines while being distributed across multiple locations or interleaved with other daily activities, reducing the prevalence of long consecutive return sequences to the same venue.

The results of this section are consistent across all CBSAs, as detailed in the Supplementary material.

Socio-demographic disparities

Finally, having identified the microscopic mechanisms whose violations are associated with deviations from the model, and how these violations are characterized from a behavioral perspective, we aim to characterize who is more prone to these patterns and, hence, at risk of not being modeled correctly. To answer this question, we test whether the deviations are related to any individual traits concerning the sociodemographics and life habits of people. Our goal is to explore whether deviations are uniformly distributed across the population or if there are specific groups that show significantly larger deviations, meaning they are less well-represented by the EPR model. Based on their inferred home census tract, users are related with sociodemographic indicators (related to wealth, education, race, and means of transportation; see Materials and methods for details) of those areas. We also get lifestyle indicators for each user based on the fraction of times they visited places of a given category, see Materials and methods for more information.

Given a sociodemographic indicator, we compute its distribution for people in the highest and lowest 10% quantiles of the ϵ_u and η_u distributions. These are users who are respectively described as the worst and best by the EPR model. In Fig. 3, we show these distributions for the sociodemographic variables of income (A), car usage (B), and the fraction of White population (C) for the two extreme quantiles of ϵ_u. The income distribution of the worst-described users in the highest 10% of ϵ_u is shifted to lower values compared to the best-described users in the lowest 10%. This implies a possible correlation between income and the ϵ_u deviation, suggesting that the EPR model predicts less accurately the mobility of people living in lower-income areas. Meanwhile, the same distributions computed for fraction of White people and car owners are less concentrated but skew toward lower values for those in the highest 10% of ϵ errors. Additionally, similar observations appear when investigating the η_u deviations (for details, see Supplementary material). These findings suggest that users poorly represented by the EPR model, in terms of both exploration dynamics and visitation frequency, are more likely to live in areas of lower income, less car ownership and less White population than those who are well-represented by the model.

To establish a more robust observation of these sociodemographic biases, not only for extreme quantiles but for all users, we perform a LASSO regression with 10-fold cross-validation. We use the deviation metrics (ϵ_u or η_u) as dependent variables, and all sociodemographic and life habit features as predictors (see Materials and methods for details). We control for S_u and K_u (respectively for ϵ_u and η_u) to avoid measuring an effect due to varying sample sizes used to compute the dependent variables. Interestingly, we achieve $R^2 = 0.20$ correlation between the observed ϵ_u and predicted $\hat{\epsilon}_u$ ($R^2 = 0.19$ for η_u, see Supplementary material), indicating that the deviations are not randomly distributed. On the contrary, they can be partially predicted by users' sociodemographic and life habit features, as seen in Fig. 3D and the Supplementary material. Similar scores are achieved for all 11 CBSAs (see Supplementary material for details).

Importantly, these associations remain qualitatively robust after conditioning for local built-environment characteristics, including nearby POI density and diversity around users' home locations (see Supplementary material). While environmental opportunity structure contributes additional explanatory power to the regression models, socioeconomic and lifestyle-related associations persist even after accounting for differences in urban accessibility and local venue diversity.

The different features ranked by their regression coefficients (in Fig. 3E) identify income as the most relevant sociodemographic characteristic in determining the ϵ error (and also η, see Supplementary material). Indeed, this significantly negative coefficient of income in both regressions verifies our earlier observation that users poorly represented by the model are more likely to live in areas of lower income. Moreover, this observation is robust across all CBSAs analyzed (for details, see Supplementary material), with income consistently showing the largest negative coefficient. Exceptions appear for η_u in New York and Los Angeles, where income has the second most negative coefficient (details in the Supplementary material). On the other hand, the coefficient for car use behaves differently for the two deviation metrics, being negatively associated with ϵ_u and positively with η_u, not only in Boston but in most CBSAs (details in Supplementary material). Interestingly, after conditioning for built-environment exposure, car usage becomes positively associated with both deviation metrics (see Supplementary material), suggesting that part of the original mixed association was confounded with differences in urban accessibility and environmental structure. Finally, contrary to our earlier conjecture, area's ethnicity does not strongly influence model performance in Boston, but it is significant in some CBSAs (details in Supplementary material). In particular, we found that areas with more Black population show less deviation from the model, indicating that people living in those areas are often more likely to be well-represented by the model.

Similar to the census variables, model deviations are also strongly biased concerning certain life habits, as shown in Fig. 3F, where we present five features with the highest and lowest coefficients. A positive coefficient for a given category indicates that users who spend a significant fraction of their time visiting that category are likely to exhibit higher deviations and, consequently, be poorly represented by the model. Conversely, a negative coefficient indicates that users who spend much of their time in that category are more likely to adhere to the model. Places like offices, factories, and buildings are primarily positively associated with larger deviations. In contrast, negatively correlated categories include restaurants like Sushi and American. In the Supplementary material, we show the results for all categories, grouping them by the macro category they

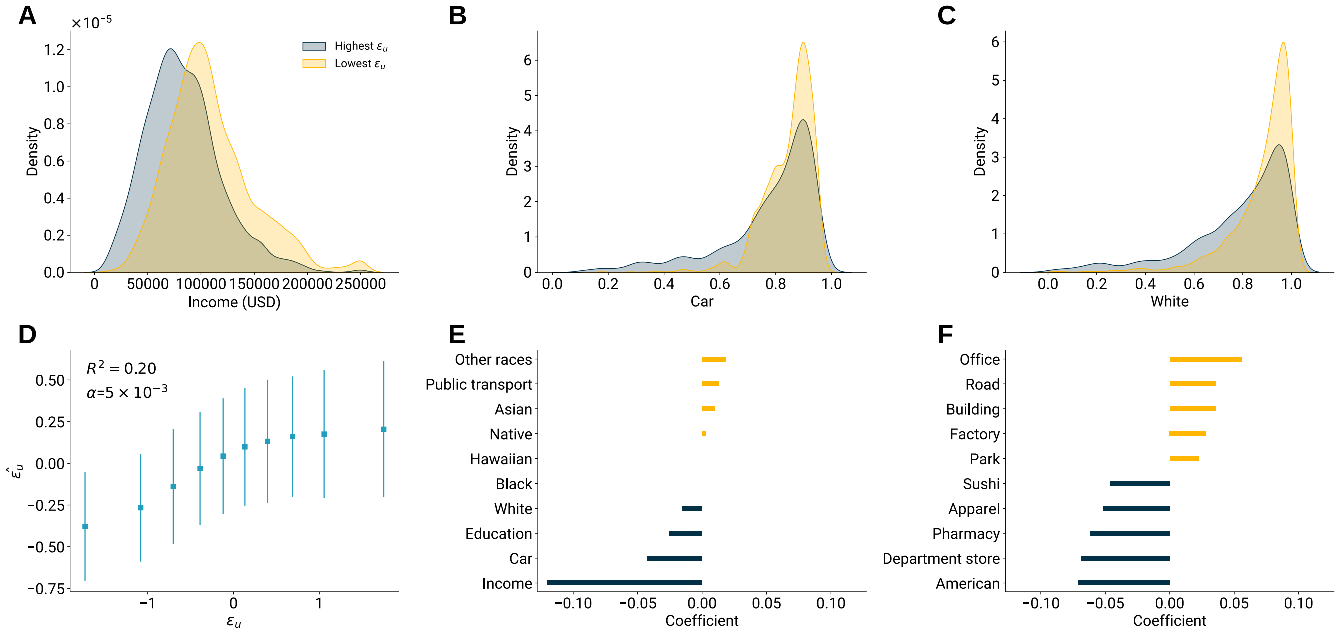

Figure 3 Deviations are biased toward sociodemographics and lifestyles. A) The income distribution of users in the highest and lowest 10% quantiles of the deviation ϵ_u. B) Same as A) for car usage. C) Same as A) for the probability of being white. D) Results of the LASSO regression: true ϵ_u vs. predicted $\hat{\epsilon_u}$ based on sociodemographic and lifestyle features. R^2 is the coefficient of determination, and α is the regularization parameter. E) Coefficients of the socioeconomic features from the LASSO regression. F) Coefficients of the life habit features (showing only the highest and lowest 5) from the LASSO regression.

are assigned to. Most place belonging to the “Food,” “Shopping”, and “Arts/Museum” macro categories are negatively related with deviations, while most places belonging to the “Work” and “City/Outdoor” macro categories are positively related with deviations. Similar patterns are observed across all CBSAs (see Supplementary material for details). Overall, these results indicate that mobility constraints and routines have a strong impact on the adherence with the EPR scaling laws: users with more work-driven daily routines, who spend more time in offices and factories, are more likely to be poorly represented by the model, while users who spend more time in restaurants, museums, and shops are less likely to experience deviations.

Discussion

Our study highlights important limitations in the universal applicability of mobility models. Despite their simplicity appeal, modeling human mobility solely based on population-wide behavior carries the risk of overlooking variations across diverse populations. By analyzing large-scale mobility data, we compared individual exploration dynamics and visitation frequency with the predictions of the EPR model, revealing significant variations in adherence that cannot be fully explained by stochasticity. These findings underscore the potential pitfalls of assuming that a single framework applies equally to all individuals. In reality, urban mobility is highly heterogeneous, influenced not only by personal preferences but also by external constraints. While unified models can offer valuable insights at the population level, it is essential to recognize that their accuracy will not be uniform across all individuals, and may be particularly poor for some specific groups.

Our results demonstrate that individuals who deviate from the EPR model share distinct behavioral patterns. They tend to visit habitual locations in consecutive sequences and rarely engage in exploration. When they do explore, it happens in short bursts, predominantly at nonroutine and amusement places. These behaviors are not randomly distributed across the population but are strongly linked to socioeconomic factors, with individuals living in lower-income areas exhibiting systematically larger deviations from the model expectations.

These findings should be interpreted while acknowledging the well-known representativeness limitations of mobile phone mobility data. Smartphone-based datasets provide partial and uneven coverage of the population, with participation and data quality varying across socioeconomic groups, demographic characteristics, and urban contexts (46–50). Such biases can affect both descriptive mobility analyses and modeling applications (51, 52). In our case, additional analyses reported in the Supplementary material show that the observed associations remain robust after accounting for income representativeness and applying representative resampling procedures. Nevertheless, these analyses address only one possible dimension of representativeness, and other sources of bias may still affect the observed mobility patterns. While such limitations are difficult to eliminate entirely in large-scale digital mobility datasets, the robustness analyses suggest that the main findings are not solely driven by uneven socioeconomic coverage in the underlying data.

A notable implication of our findings is the unequal spatial accuracy of the EPR model. As shown in Fig. 4, users better represented by the model tend to live in less densely populated suburban and rural areas. In contrast, those with the highest deviations are concentrated in densely populated urban environments (see Supplementary material for details). This spatial pattern is a combination of resident residential segregation by income, with wealthier individuals typically residing outside city centers, and our finding that the model perform better in those areas. Interestingly, while the EPR model is designed to simulate urban mobility, performs better in suburban and

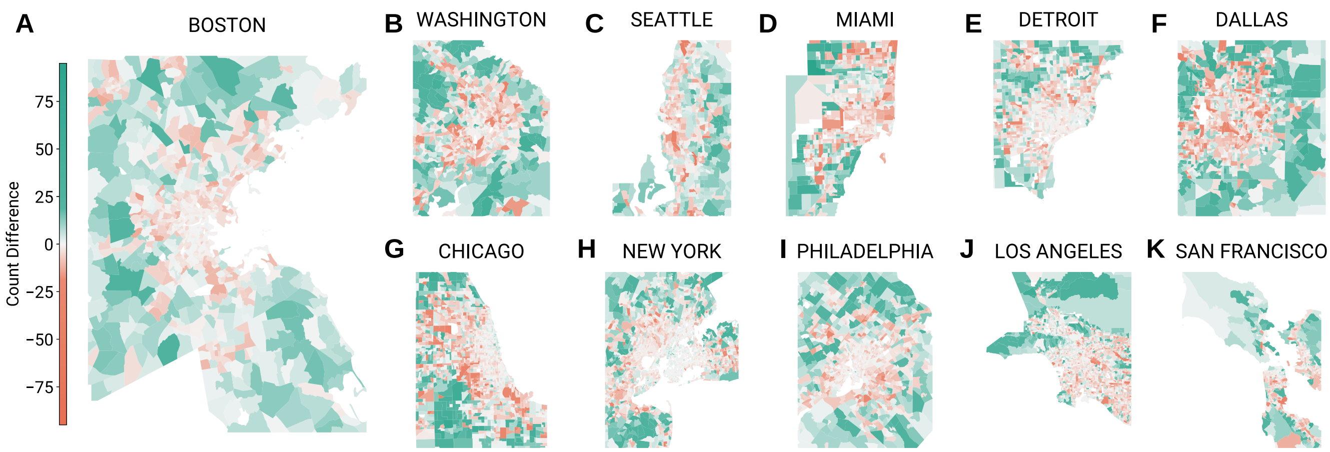

Figure 4 Urban–suburban/rural divide. A–K) US census tracts division of the 11 CBSAs under consideration, where each tract is colored according to the difference count between the number of users in the highest and lowest 10% of $\epsilon_u + \eta_u$ with estimated home location in the tract.

exurban/rural settings where movement patterns are more predictable. More broadly, the spatial and behavioral dimensions associated with these deviations may also connect to questions concerning opportunity exposure and long-term social mobility across neighborhoods (53–55), although investigating these connections directly lies beyond the scope of the present work.

From a broader modeling perspective, our findings suggest that the main limitation of universal mobility frameworks may not lie in their aggregate predictive power, but in the implicit assumption that model uncertainty is uniformly distributed across the population. In reality, deviations are structured, behaviorally meaningful, and socially stratified. This does not invalidate the importance or practical usefulness of these models. Rather, it highlights the importance of explicitly characterizing where and for whom model assumptions become less accurate. Depending on the application, incorporating additional mechanisms related to burstiness, recency or routine may help reduce some of the observed deviations.

These considerations are particularly relevant in dense urban environments, where mobility models are most commonly applied and where our results reveal the largest deviations from the EPR framework. As mobility models become increasingly integrated into transportation planning, accessibility analysis, epidemic modeling, and infrastructure design, uneven predictive accuracy across social groups may become increasingly important to understand and communicate (34–36, 56, 57). This perspective parallels the growing attention devoted to biases in digital mobility datasets: just as mobile phone data are widely used despite known representativeness limitations, mobility models may also need to be interpreted with awareness of their structured and nonuniform uncertainties. Understanding how model uncertainty is distributed across populations and urban contexts may become a central challenge for future mobility modeling.

Materials and methods

Data

Our privacy-enhanced geo-location data, provided by Cuebiq, consists of anonymized GPS records ("pings") from users who opted in through a GDPR and CCPA-compliant framework. Collected in 2017 under Cuebiq's Data for Good program, the data is used for academic research and humanitarian purposes. The dataset includes pings from 11 core-based statistical areas (CBSAs) between October 2016 and March 2017: New York, Los Angeles, Chicago, Dallas, Philadelphia, Washington, Miami, Boston, San Francisco, Detroit, and Seattle. The original 70.2 billion pings from 14.3 million smartphones were filtered to 67 billion pings from 4.5 million smartphones by considering only devices with over 2,000 pings. Using the Hariharan and Toyama algorithm (58), we extracted stays from location trajectories and identified venues within a 200-m radius. Stays under 5 min or over 1 day were discarded. Home locations were inferred from the most common location (expressed in terms of Census Block Group) between 10:00 PM and 6:00 AM, further refining the data to 976 million stays from 3.6 million individuals. Excluding users with <10 nights spent in their inferred home location or without visits to our set of venues, we are left with 1.9 million users. Finally, discarding the lowest quintile in terms of the number of distinct visited places, the final dataset includes visits from 1.5 million users with at least 11 unique visited places. Refer to Ref. (6) for full details on privacy protection, visits extraction, and post-stratification techniques. Additional analyses on sampling bias, representativeness across income groups, and robustness under income-balanced resampling are reported in the Supplementary material. The use of this anonymized mobility dataset was reviewed and approved by Northeastern University IRB committee (protocol IRB 24-03-43).

Exploration tendency

The exploration tendency parameter ρ_u of a user u is given by:

$$\rho_u = \frac{S_u^{\gamma+1}}{(\gamma+1)N_u},$$

where S_u is the total number of distinct places, and N_u is the total number of places visited by the user.

Expected inter-event time

Since at every step the probability of visiting a new place for a user u is given by $P_u(S) = \rho_u S^{-\gamma}$, the probability that the next exploration step will occur after T steps is given by:

$$P(\tau_{u,S} = T) = (1 - P_u(S))^{T-1} P_u(S),$$

which is a geometric distribution with expected value $\langle \tau_{u,S} \rangle$ given by $\langle \tau_{u,S} \rangle = P_u^{-1}(S) = S^\gamma/\rho_u$.

Sociodemographic indicators

Each user in our data set is assigned a Census Block Group, as measured by the 2012–2016 5-year American Community Survey (59) (ACS), as an inferred home location, using its most common location between 10:00 PM and 6:00 AM. From the same ACS data, we assign the user sociodemographic variables taken or calculated from its home Census Block Group indicators:

- Income: median household income
- Car, Public transport: fraction of the population who take a given means of transportation (we consider only car and public transport) to commute
- Education: fraction of the population with a higher education degree
- White, Black, Asian, Hawaiian, Other races: fraction of the population who identifies with a given ethnicity or race.

Life habit indicators

Visits in the clean data set are associated with a Foursquare venue and its category. Venue categories are taken from the Foursquare classification (42). Moreover, categories have been manually grouped into 13 macro groups (6): Art/Museum, City/Outdoors, Coffee/Tea, College, Entertainment, Food, Grocery, Health, Service, Shopping, Sports, Transportation, Work. We assign each user a category score for each of the 592 Foursquare categories, based on the fraction of visits spent in places classified in each category.

Regression model

To test the bias of the EPR model toward sociodemographic and life habit indicators, we run a regression model using either ϵ_u or η_u as the dependent variable and the full list of sociodemographic and life habit variables as independent variables. Moreover, we also include S_u and K_u, respectively for ϵ_u and η_u, as control variables, as they indicate the number of elements in the sum of either ϵ_u or η_u, respectively. Given the high number of features (one control, 10 sociodemographic, 592 for life habits), we consider a Least Absolute Shrinkage and Selection Operator (LASSO) regression, whose objective function is:

$$\min_{\beta} \left(\sum_{i=1}^{n} (y_i - \beta_0 - \sum_{j=1}^{p} \beta_j x_{ij})^2 + \alpha \sum_{j=1}^{p} |\beta_j| \right),$$

where y_i is the dependent variable, β_i's are the coefficients, x_{ij} are the independent variables and α is the regularization parameter. There are numerous reasons to use this type of model in our case. Indeed, through the regularization parameter α, it performs automatic feature selection by shrinking the least important coefficients to zero, thus handling multicollinearity and preventing overfitting at the same time. We estimate the parameter α through 10-fold cross-validation with 3 repeated randomizations. All variables, including the dependent ones, have being standardized by substructing the mean and scaling to unit variance.

Exploration burstiness

Having the sequence of exploration inter-event times $\{\tau_{u,S}\}$ of a user u with N_u total visits, we can compute the burstiness coefficient B_u for finite sequences as defined in (44):

$$B_u = \frac{\sqrt{N_u + 1}r - \sqrt{N_u - 1}}{(\sqrt{N_u + 1} - 2)r + \sqrt{N_u - 1}},$$

where $r = \sigma(\tau_{u,S})/\mu(\tau_{u,S})$ is the coefficient of variation (σ and μ are, respectively, the empirical SD and mean of the $\{\tau_{u,S}\}$ sequence.

Biased return

To measure the extent to which a user respects the preferential return principle, we measure individually the empirical deviation from the equation $\Pi_i = \phi_i$, where Π_i is the probability of returning to a location i and ϕ_i is the fraction of previous visits to that location. To do so, we bin ϕ (which is a continuous variable defined in (0, 1]) in 20 discrete and equally spaced ϕ_b intervals ((0., 0.05], (0.05, 0.1],..., (0.95, 1]), and for every user we build a list of empirical realizations Π_{ϕ_b} for every bin ϕ_b, in the following way: at every return step, we recompute ϕ_i for each previously visited location i and map it to the respective bin ϕ_b; then, we add a 1 to the Π_{ϕ_b} list of the location to which the user actually returns, and 0 to the lists of all the others (if any). After repeating the procedure for all return steps, we compute the empirical probability $\tilde{\Pi}_{\phi_b}$ as the empirical average of the binary values in Π_{ϕ_b}, for every bin ϕ_b. $\tilde{\Pi}_{\phi_b}$ indicates the observed fraction of times the user returned to places previously visited with frequency ϕ_b. Finally, we can compute how different $\tilde{\Pi}_{\phi_b}$ is from ϕ_b, defining the biased return R_u as the symmetrical mean absolute percentage error (SMAPE) of $\tilde{\Pi}_{\phi_b}$ from the expected value ϕ_b:

$$R_u = \frac{1}{20} \sum_{b=1}^{20} \frac{|\tilde{\Pi}_{\phi_b} - \phi_b|}{|\tilde{\Pi}_{\phi_b}| + |\phi_b|}.$$

Taxonomy of bursty trains

A bursty train is a sequence of consecutive exploration steps of length >1. Considering only the steps belonging to a bursty train of any user and a taxonomy category χ, we define $f_B(\chi)$ as the portion of those steps that are visits to the category χ. Similarly, considering all the exploration steps of any user, we define $f_e(\chi)$ as the portion of those steps that are visits to the category χ. Finally, considering all the steps of any user, we define $f(\chi)$ as the portion of those steps that are visits to the category χ. The blue and red bars in Fig. 2C refer, respectively, to the relative frequencies $\tilde{f}_B(\chi) = (f_B(\chi) - f(\chi))/f(\chi)$ and $\tilde{f}_{B,e}(\chi) = (f_B(\chi) - f_e(\chi))/f_e(\chi)$.

Taxonomy of recency trains

A recency train is a sequence of consecutive return steps to the same exact venue, of length greater than one. Considering only the steps belonging to a recency train of any user and a taxonomy category χ, we define $f_R(\chi)$ as the portion of those steps that are visits to the category χ. Similarly, considering all the return steps of any user, we define $f_r(\chi)$ as the portion of those steps that are return visit to the category χ. Finally, $f(\chi)$ has already been defined as the portion of all steps that are visits to the category χ. The blue and red bars in Fig. 2D refer, respectively, to the relative frequencies $\tilde{f}_R(\chi) = (f_R(\chi) - f(\chi))/f(\chi)$ and $\tilde{f}_{R,r}(\chi) = (f_R(\chi) - f_r(\chi))/f_r(\chi)$.

Acknowledgments

We are thankful to Takahiro Yabe for insightful comments.

Supplementary Material

Supplementary material is available at *PNAS Nexus* online.

Competing Interest

The authors declare no competing interests.

Funding

E.M. acknowledges support from the US National Science Foundation under grants 2420945 and 2427150. M.K. acknowledges funding from the National Laboratory for Health Security (RRF-2.3.1-21-2022-00006); the DATAREDUX (ANR-19-CE46-0008); the SoBigData++ PPP HORIZON-INFRA-2021-DEV-02 no. 101079043; the DUT-FFG COLINE; and the MOMA WWTF projects. L.N. and M.K. were supported by the NSF AccelNet-MultiNet program under grant no. 1927425.

Author Contributions

L.N., M.K., and E.M. designed the research; L.N. performed research; L.N. and E.M. analyzed the data; L.N., M.K., and E.M. wrote the article.

Preprints

This manuscript was posted on a preprint: https://arxiv.org/abs/2410.23502.

Data Availability

The mobility data that support the findings of this study are available from Spectus through their Social Impact program https://spectus.ai/social-impact/, but restrictions apply to the availability of these data, which were used under the license for the current study and are therefore not publicly available. Data access requests should be submitted through Spectus' Social Impact customer page via https://cuebiq.com/demo/, where the sales team at Spectus may be contacted in a timely manner. Anonymized and aggregated data and code to reproduce the results of our article can be found at https://github.com/ludoviconapoli/deviations-from-universality.

References

1. Kitamura R, Chen C, Pendyala RM, Narayanan R. 2000. Micro-simulation of daily activity-travel patterns for travel demand forecasting. *Transportation*. 27:25–51.
2. Barthelemy M. *The structure and dynamics of cities*. Cambridge University Press, 2016.
3. Wang A, *et al.* 2020. A review of human mobility research based on big data and its implication for smart city development. *ISPRS Int J Geoinf*. 10:13.
4. Nagel K, Paczuski M. 1995. Emergent traffic jams. *Phys Rev E*. 51:2909–2918.
5. Çolak S, Lima A, González MC. 2016. Understanding congested travel in urban areas. *Nat Commun*. 7:10793.
6. Moro E, Calacci D, Dong X, Pentland A. 2021. Mobility patterns are associated with experienced income segregation in large US cities. *Nat Commun*. 12:1–10.
7. Xu F, *et al.* 2025. Using human mobility data to quantify experienced urban inequalities. *Nat Hum Behav*. 9:654–664.
8. Balcan D, *et al.* 2009. Multiscale mobility networks and the spatial spreading of infectious diseases. *Proc Natl Acad Sci U S A*. 106:21484–21489.
9. Tizzoni M, *et al.* 2014. On the use of human mobility proxies for modeling epidemics. *PLoS Comput Biol*. 10:Article e1003716.
10. Barbosa H, *et al.* 2018. Human mobility: models and applications. *Phys Rep*. 734:1–74.
11. Brockmann D, Hufnagel L, Geisel T. 2006. The scaling laws of human travel. *Nature*. 439:462–465.
12. Alessandretti L, Aslak U, Lehmann S. 2020. The scales of human mobility. *Nature*. 587:402–407.
13. Zipf GK. 1946. The P_1P_2/D hypothesis: on the intercity movement of persons. *Am Sociol Rev*. 11:677–686.
14. Simini F, González MC, Maritan A, Barabási A-L. 2012. A universal model for mobility and migration patterns. *Nature*. 484:96–100.
15. Schläpfer M, *et al.* 2021. The universal visitation law of human mobility. *Nature*. 593:522–527.
16. Erlander S, Stewart NF. 1990. *The gravity model in transportation analysis: theory and extensions*. Vol. 3. VSP, 1990.
17. Simini F, Barlacchi G, Luca M, Pappalardo L. 2021. A deep gravity model for mobility flows generation. *Nat Commun*. 12:6576.
18. Toole JL, Herrera-Yaqüe C, Schneider CM, González MC. 2015. Coupling human mobility and social ties. *J R Soc Interface*. 12: 20141128.
19. Montroll EW, Weiss GH. 1965. Random walks on lattices. II. *J Math Phys*. 6:167–181.
20. Song C, Koren T, Wang P, Barabási A-L. 2010. Modelling the scaling properties of human mobility. *Nat Phys*. 6:818–823.
21. Gonzalez MC, Hidalgo CA, Barabasi A-L. 2008. Understanding individual human mobility patterns. *Nature*. 453:779–782.
22. Song C, Qu Z, Blumm N, Barabási A-L. 2010. Limits of predictability in human mobility. *Science*. 327:1018–1021.
23. Pappalardo L, Rinzivillo S, Simini F. 2016. Human mobility modelling: exploration and preferential return meet the gravity model. *Procedia Comput Sci*. 83:934–939.
24. Barbosa H, de Lima-Neto FB, Evsukoff A, Menezes R. 2015. The effect of recency to human mobility. *EPJ Data Sci*. 4:1–14.

25. Jiang S, *et al.* 2016. The timegeo modeling framework for urban mobility without travel surveys. *Proc Natl Acad Sci U S A*. 113:E5370–E5378.
26. Pappalardo L, *et al.* 2015. Returners and explorers dichotomy in human mobility. *Nat Commun*. 6:8166.
27. Pappalardo L, Simini F. 2018. Data-driven generation of spatio-temporal routines in human mobility. *Data Min Knowl Discov*. 32:787–829.
28. Xu Y, Belyi A, Bojic I, Ratti C. 2018. Human mobility and socioeconomic status: analysis of Singapore and Boston. *Comput Environ Urban Syst*. 72:51–67.
29. Leo Y, Fleury E, Alvarez-Hamelin JI, Sarraute C, Karsai M. 2016. Socioeconomic correlations and stratification in social-communication networks. *J R Soc Interface*. 13:20160598.
30. Lotero L, Hurtado RG, Mario Floría L, Gómez-Gardeñes J. 2016. Rich do not rise early: spatio-temporal patterns in the mobility networks of different socio-economic classes. *R Soc Open Sci*. 3:150654.
31. Barbosa H, *et al.* 2021. Uncovering the socioeconomic facets of human mobility. *Sci Rep*. 11:8616.
32. Millanida Hilman R, Iñiguez G, Karsai M. 2022. Socioeconomic biases in urban mixing patterns of US metropolitan areas. *EPJ Data Sci*. 11:32.
33. Dong X, *et al.* 2020. Segregated interactions in urban and online space. *EPJ Data Sci*. 9:20.
34. Gozzi N, *et al.* 2021. Estimating the effect of social inequalities on the mitigation of COVID-19 across communities in Santiago de Chile. *Nat Commun*. 12:1–9.
35. Pullano G, Valdano E, Scarpa N, Rubrichi S, Colizza V. 2020. Evaluating the effect of demographic factors, socioeconomic factors, and risk aversion on mobility during the COVID-19 epidemic in France under lockdown: a population-based study. *Lancet Digit Health*. 2:e638–e649.
36. Dueñas M, Campi M, Olmos LE. 2021. Changes in mobility and socioeconomic conditions during the COVID-19 outbreak. *Humanit Soc Sci Commun*. 8:1–10.
37. Napoli L, Sekara V, García-Herranz M, Karsai M. 2023. Socioeconomic reorganization of communication and mobility networks in response to external shocks. *Proc Natl Acad Sci U S A*. 120:Article e2305285120.
38. Yang Y, Pentland A, Moro E. 2023. Identifying latent activity behaviors and lifestyles using mobility data to describe urban dynamics. *EPJ Data Sci*. 12:15.
39. Schönfelder S, Axhausen KW. 2003. Activity spaces: measures of social exclusion? *Transp Policy*. 10:273–286.
40. Susilo YO, Axhausen KW. 2014. Repetitions in individual daily activity–travel–location patterns: a study using the Herfindahl–Hirschman index. *Transportation*. 41:995–1011.
41. United States Census Bureau. 2020. Core-based statistical areas. https://www.census.gov/programs-surveys/metro-micro/about.html.
42. Foursquare Venue Category Hierarchy. 2020. https://developer.foursquare.com/docs/build-with-foursquare/categories/.
43. Karsai M, Jo H-H, Kaski K. *Bursty human dynamics*. Springer, 2018.
44. Kim E-K, Jo H-H. 2016. Measuring burstiness for finite event sequences. *Phys Rev E*. 94:032311.
45. Barabási A-L, Albert R. 1999. Emergence of scaling in random networks. *Science*. 286:509–512.
46. Wesolowski A, Eagle N, Noor AM, Snow RW, Buckee CO. 2013. The impact of biases in mobile phone ownership on estimates of human mobility. *J R Soc Interface*. 1020120986.
47. Omodei E, Garcia-Herranz M, Paolotti D, Tizzoni M. 2022. Complex systems for the most vulnerable. *J Phys Complex*. 3:021001.
48. Zhao Z, *et al.* 2016. Understanding the bias of call detail records in human mobility research. *Int J Geograph Inf Sci*. 30:1738–1762.
49. Sinclair M, *et al.* 2023. Assessing the socio-demographic representativeness of mobile phone application data. *Appl Geogr*. 158:102997.
50. Li Z, Ning H, Jing F, Lessani MN. 2024. Understanding the bias of mobile location data across spatial scales and over time: a comprehensive analysis of safegraph data in the United States. *PLoS One*. 19:Article e0294430.
51. Schlosser F, *et al.* 2020. COVID-19 lockdown induces disease-mitigating structural changes in mobility networks. *Proc Natl Acad Sci U S A*. 117:32883–32890.
52. Sekara V, *et al.* 2024. The opportunities, limitations, and challenges in using machine learning technologies for humanitarian work and development. *Adv Complex Syst (ACS)*. 27:1–16.
53. Chetty R, Hendren N. 2018. The impacts of neighborhoods on intergenerational mobility I: childhood exposure effects. *Q J Econ*. 133:1107–1162.
54. Chetty R, Hendren N. 2018. The impacts of neighborhoods on intergenerational mobility II: county-level estimates. *Q J Econ*. 133:1163–1228.
55. Sharkey P, Faber JW. 2014. Where, when, why, and for whom do residential contexts matter? Moving away from the dichotomous understanding of neighborhood effects. *Annu Rev Sociol*. 40:559–579.
56. Verma S. 2019. Weapons of math destruction: how big data increases inequality and threatens democracy. *Vikalpa*. 44:97–98.
57. Mena GE, *et al.* 2021. Socioeconomic status determines COVID-19 incidence and related mortality in Santiago, Chile. *Science*. 372:Article eabg5298.
58. Hariharan R, Toyama K. 2004. Project lachesis: parsing and modeling location histories. In: *International Conference on Geographic Information Science*. Springer. p. 106–124.
59. U.S. Census Bureau. 2017. 2016 American community survey 5-year data. https://www.census.gov/programs-surveys/acs.